JOURNAL OF GEOPHYSICAL RESEARCH, VOL. 108, NO. D14, 4402, doi:10.1029/2002JD003220, 2003

A parameterization of cirrus cloud formation: Heterogeneous freezing

B. Kärcher

Deutsches Zentrum für Luft- und Raumfahrt, Oberpfaffenhofen, Institut für Physik der Atmosphäre, Wessling, Germany

U. Lohmann

Department of Physics and Atmospheric Science, Dalhousie University, Halifax, Nova Scotia, Canada

Received 26 November 2002; revised 12 February 2003; accepted 18 March 2003; published 16 July 2003.

[1] A physically based parameterization of cirrus cloud formation by heterogeneous freezing is developed along with a novel method to compute associated nucleation rates. The analysis is restricted to immersion freezing, possibly the dominant pathway for heterogeneous cirrus formation under cold (<235 K) conditions. The size of ice nuclei (IN) immersed in a liquid particle does not significantly affect the heterogeneous freezing threshold (the saturation ratio over ice where ice formation is initiated) of the mixed particle. If perfect IN were present at cirrus altitudes, almost all of them would freeze near ice saturation, even in slow updrafts. If only one type of less potent IN with freezing thresholds >1.3–1.4 triggers cirrus formation, cloud properties are not very susceptible to changes of IN properties, as in the case of homogeneous freezing. In contrast, much stronger indirect aerosol effects on cirrus clouds are possible if at least two types of IN with distinct freezing thresholds compete during the freezing process, most likely leading to a suppression of ice crystal concentrations. *INDEX TERMS:* 0305 Atmospheric Composition and Structure: Aerosols and particles (0345, 4801); 0320 Atmospheric Composition and Structure: Cloud physics and chemistry; 0365 Atmospheric Composition and Structure: Troposphere—composition and chemistry; *KEYWORDS:* aerosols, ice nucleation, cirrus clouds, parameterization, ice nuclei, freezing

Citation: Kärcher, B., and U. Lohmann, A parameterization of cirrus cloud formation: Heterogeneous freezing, *J. Geophys. Res.*, *108*(D14), 4402, doi:10.1029/2002JD003220, 2003.

1. Introduction

1.1. Evidence for Heterogeneous Freezing

[2] The relevance of homogeneous freezing of supercooled aerosols has been emphasized in numerous studies of cirrus cloud formation [*Heymsfield and Sabin*, 1989; *Sassen and Dodd*, 1989; *Jensen and Toon*, 1992; *Heymsfield and Miloshevich*, 1993; *Jensen et al.*, 1998; *Lin et al.*, 1998; *Spice et al.*, 1999; *Field et al.*, 2001; *Möhler et al.*, 2003]. Most studies have revealed that orographic ice clouds predominantly form at rapid cooling rates, leading to large supersaturations with respect to ice at temperatures below ~235 K and rendering homogeneous freezing the most likely ice particle formation mechanism for this type of cloud. A comprehensive comparison of microphysical simulations with freezing measurements carried out in an aerosol chamber approximating real cirrus cloud formation has shown that the activity-based parameterization of homogeneous ice nucleation rates provided by *Koop et al.* [2000a] can be employed to simulate the formation of cirrus clouds by this process [*Haag et al.*, 2003].

[3] The presence of heterogeneous ice-forming nuclei may reduce the energy barrier for the nucleation of ice germs and thereby facilitate the formation of the new phase. Some information is available on the nature and properties of ice nuclei (IN) that cause the formation of mixed-phase clouds (forming by freezing of metastable water drops) [*Vali*, 1985a; *Pruppacher and Klett*, 1997]. However, it remains unclear under which atmospheric conditions heterogeneous freezing of aerosols leads to the formation of cold cirrus clouds (forming by freezing of supercooled aerosols) [*DeMott*, 2002]. This is caused by the lack of information about the origin, spatial distribution, and chemical nature of the IN in the upper troposphere [*Kärcher and Solomon*, 1999], by the lack of a basic theoretical description of heterogeneous nucleation, and by experimental limitations to measure IN at high altitudes. Well-conceived case studies, as in the case of wave cirrus, are not available, except for mixed-phase clouds.

[4] A collection of aircraft data suggests that freezing in midlatitude cirrus could be initiated at ice saturation ratios lower than caused by homogeneous freezing (i.e., <1.4–1.7 or <140–170% when expressed as relative humidities over ice) [*Heymsfield et al.*, 1998]. Other available data have been summarized by *Martin* [2000]. The column of air that freezes homogeneously at high supersaturations during

0148-0227/03/2002JD003220$09.00

adiabatic ascent would be thicker than observed mean vertical thicknesses (<0.5–1 km) of optically thin and subvisible cirrus clouds [*Sassen and Cho*, 1992; *Winker and Trepte*, 1998], rendering homogeneous freezing as the main formation path unlikely. A theoretical study has pointed out that subvisible cirrus are likely to be formed by IN (if present) at low temperatures and in weak updrafts, although liquid aerosol particles might be far more abundant [*Kärcher*, 2002].

[5] More recent evidence for heterogeneous freezing taking place in the upper troposphere and tropopause region has been reported based on field measurements. An analysis of aerosol particles remaining from evaporated cirrus crystals showed that the freezing fraction of the aerosol did not show the characteristic size dependence expected for pure homogeneous freezing [*Seifert et al.*, 2002].

1.2. Measuring Heterogeneous Freezing Thresholds

[6] In this paper we define the freezing threshold as the saturation ratio over ice where the first ice particles nucleate. This quantity is not sharply defined as it depends on the size of the freezing particles and on the timescale of the freezing event, among other factors. It can be calculated if an expression for the nucleation rate is known (as done in this work), or it can be determined from measurements. Conventionally, measured and calculated freezing thresholds are compared under conditions where the (calculated and observed) nucleation rates generate one ice particle in 1 s.

[7] A review of laboratory methodologies and results of laboratory studies of ice formation has been given by *DeMott* [2002]. Many of the studies addressed in the review investigated heterogeneous ice nucleation under thermodynamic conditions different from those prevailing at cirrus levels or used particles with sizes and/or chemical compositions that are rather untypical for atmospheric aerosols.

[8] Particles relevant to cirrus formation include black carbon soot and, perhaps, organic carbon, mineral dust coated with or immersed in aqueous sulfuric acid and/or organic droplets, partially deliquesced ammoniated sulfates, and sea salt. Besides sulfates and carbon, organic components are ubiquitous throughout the troposphere [*Murphy et al.*, 1998]. Sources of soot include aircraft exhaust, fossil fuel combustion, and biomass burning [*Cooke and Wilson*, 1996]. Mineral dust particles contain a variety of crustal material derived from surface sources [*Chen et al.*, 1998]. Single-particle analyses have shown that silicates and carbonaceous material are more often found in ice-forming nuclei than in aerosols not acting as IN [*Chen et al.*, 1998]. Salt crystallization in ammoniated aerosols above ice saturation may trigger heterogeneous freezing [*Tabazadeh and Toon*, 1998]. Sea-salt aerosols from the accumulation mode may be transported into the upper troposphere over oceans, but there is currently no robust experimental evidence available to support this conjecture.

[9] Recent field measurements demonstrate that ambient concentrations of nonvolatile condensation nuclei in the tropopause region are $\sim$35 cm^{-3} (northern midlatitudes) and 12 cm^{-3} (southern midlatitudes) [*Minikin et al.*, 2003]. In concert with earlier observations that revealed concentrations of effective IN as high as 0.1 cm^{-3} in the continental upper troposphere [*Rogers et al.*, 1998], this demonstrates the potential for insoluble particles from natural and anthropogenic sources to influence the formation of cirrus clouds. In fact, many of the above mentioned aerosol species have been found as inclusions in cirrus and contrail crystals [*Heintzenberg et al.*, 1996; *Ström and Ohlsson*, 1998; *Twohy and Gandrud*, 1998].

[10] The first measurements of the freezing of polydisperse black carbon (BC) particles (average diameter 240 nm) in cirrus conditions have been reported by *DeMott et al.* [1999]. While untreated BC particles triggered ice nucleation after saturation with liquid water was reached, BC particles treated with sulfuric acid caused efficient ice formation when the acid coating exceeded several percent of the particle mass and when the temperature was <220 K. In the range between 210 and 220 K the freezing occurred at relative humidities between 135 and 145%, i.e., some 10% below the homogeneous limit. This study underlines that chemical processing can be an important factor in regulating the freezing behavior of atmospheric soot particles.

[11] Heterogeneous freezing temperatures of ice in ammonium sulfate particles with mineral dust inclusions was measured in the laboratory [*Zuberi et al.*, 2002]. In the temperature regime from 198 to 239 K, threshold ice supersaturations for kaolinite and montmorillonite, two main components of the tropospheric dust aerosol, range between 1.35 and 1.51. Depending on the water activity of the aerosol, the corresponding enhancement of the homogeneous freezing temperature varies between 8 and 20 K. According to these measurements, mineral dust internally mixed with sulfates may significantly impact cirrus cloud formation, depending on its availability in the upper troposphere. Similar conclusions about the potentially important role for mineral dusts as initiators of cirrus cloud formation have been drawn by *Hung et al.* [2003] on the basis of their laboratory studies.

[12] Crystallized salts in the aerosol may act as sites for heterogeneous ice nucleation. A laboratory study investigated the possibility that ice nucleation is triggered by solid inclusions of crystalline $(NH_4)_2SO_4$ immersed in supercooled $(NH_4)_2SO_4/H_2O$ solutions and by solid inclusions of crystalline letovicite immersed in supercooled $(NH_4)HSO_4/H_2O$ solutions [*Zuberi et al.*, 2001]. The saturation ratios for heterogeneous freezing were close to unity when the solid cores were present as microcrystals. They were close to homogeneous values when the solid cores were present in the form of large crystals. This work suggests that the morphology and the thermal history of the ice-nucleating crystals might play a key role in determining the freezing behavior of deliquescing aerosols.

[13] Sea-salt particles are a complex mixture of many different ionic species dissolved in water. In the polar marine boundary layer, sea salt is mostly present in the liquid state [*Koop et al.*, 2000b]. This likely holds for sea-salt particles transported into the upper troposphere, so their potential to alter cirrus formation is probably small. This conjecture is in agreement with the known fact that maritime air masses are consistently deficient in IN and that concentrations of sea salt and IN are often observed to be anticorrelated [*Pruppacher and Klett*, 1997].

[14] It is questionable whether a significant amount of very potent IN, deriving from surface sources such as pollen [*Diehl et al.*, 2001] reaches the cirrus levels; it is conceiv-

able that such IN are mostly removed by precipitation scavenging.

1.3. Parameterizing Heterogeneous Freezing Processes

[15] Numerical studies suggest that heterogeneous freezing has the greatest impact on calculated cirrus cloud properties for low updraft speeds [*DeMott et al.*, 1997; *Spice et al.*, 1999], especially for the special class of subvisible cirrus [*Kärcher*, 2002]. The main effect of efficient IN is to lower the threshold relative humidity for cirrus formation. As low supersaturations occur more frequently and within larger atmospheric regions than higher supersaturations, the spatial extent and frequency of occurrence of heterogeneously formed clouds would be greater than in the case of the homogeneous formation mechanism.

[16] The possibility that cirrus cloud formation may, at times, be influenced, or even controlled, by aerosol particles acting as IN, as outlined in section 1.1, motivates the development of a cirrus parameterization scheme that includes heterogeneous nucleation. Most work dealing with heterogeneous ice formation, including climate models [*Lohmann*, 2002], employed prescribed IN activation spectra, based on either temperature, where the IN number density behaves as $n_{\mathrm{IN}} \propto \exp(-\beta \Delta T)$, with $\Delta T = T - 273.15$ K [*Fletcher*, 1962], on supersaturation, with $n_{\mathrm{IN}} \propto (S_i - 1)^{\beta}$ [*Wallace and Hobbs*, 1977], or on combinations thereof [*Cotton et al.*, 1986]. These equations have been employed with different values of the numerical coefficients but have been validated only by measurements at ground level or up to the midtroposphere at temperatures above ~250 K. While they might be useful to study the role of IN in rain formation in warm clouds, they may lead to unrealistically high values for n_{IN} when extrapolated to low temperatures or to high supersaturations when no special care is taken. Furthermore, these expressions do not provide a link to the dynamical forcing mechanism creating the supersaturated state.

[17] *DeMott et al.* [1997, 1998] used an effective freezing temperature determined experimentally to parameterize the effect of IN on the freezing process. Another parameterization for heterogeneous nucleation relies on the classical theory of nucleation [*Khvorostyanov and Curry*, 2000], the applicability of which is debatable [*Pruppacher and Klett*, 1997]. Numerical simulations of heterogeneous freezing prescribed the IN spectrum, based on either an extrapolation of laboratory IN data collected at ~238–248 K to lower temperatures [*DeMott et al.*, 1998] or on a modified Fletcher function [*Sassen and Benson*, 2000]. A relationship for the number density of ice crystals after a given time as a function of the physical parameters driving the freezing process has not been provided.

[18] We have developed such a physically based parameterization scheme for homogeneous freezing [*Kärcher and Lohmann*, 2002a, 2002b] and presented first applications of it in a general circulation model [*Lohmann and Kärcher*, 2002, 2003]. It is the main goal of the present work to provide an extension of the parameterization that includes heterogeneous processes without making use of the concepts of the classical nucleation theory. Furthermore, we provide an expression to calculate heterogeneous nucleation rates for mixed particles based on shifts of the water activity in freezing particles (or relative humidity) and discuss important atmospheric implications.

2. Theoretical Framework

[19] The basic theoretical description of the parameterization scheme is very similar to the homogeneous case presented in detail by *Kärcher and Lohmann* [2002b], treating freezing and the initial growth of ice particles in an adiabatic ascent with prescribed constant vertical velocity. Only the key equations are recalled in section 2.1. The main difference between the homogeneous scheme and the heterogeneous scheme concerns the treatment of the freezing thresholds and freezing modes, and these aspects are discussed in sections 2.2 and 2.3.

2.1. Basic Equations

2.1.1. Characteristic Timescales

[20] The physics of ice initiation in cirrus is largely controlled by two distinct timescales [*Kärcher and Lohmann*, 2002a, 2002b]. The characteristic timescale τ of the freezing event can be related to the cooling rate $dT/dt > 0$ of the air parcel (which is strictly proportional to the updraft speed w when the air parcel rises adiabatically) by

$$\tau^{-1} = c \left(\left| \frac{\partial \ln(J)}{\partial T} \right| \right)_{S_i = S_{cr}} \frac{dT}{dt}, \tag{1}$$

where c is a constant determined with the help of numerical simulations of the freezing process and where the bracketed term is the derivative of the logarithm of the freezing rate coefficient J taken at the freezing threshold saturation ratio over ice, $S_i = S_{cr}$. (Throughout this work, we will use the term rate for J for simplicity, although the term rate coefficient is more appropriate as J denotes the number of ice germs produced per cm^3 of droplet volume per unit time for homogeneous freezing and per cm^2 of IN surface area per unit time for heterogeneous freezing.)

[21] The initial growth timescale τ_g and the dimensionless parameter δ are defined by

$$\tau_g^{-1} = b_1 b_2 \frac{1/\delta}{1+\delta}, \quad \delta = b_2 r_0 \tag{2}$$

where $b_1 = v \alpha v_{th} n_{\mathrm{sat}} (S_i - 1)/4$ and $b_2 = \alpha v_{th}/(4D)$ are coefficients entering the single ice particle (radius r_i, initial value r_0) growth law $dr_i/dt = b_1/(1 + b_2 r_i)$. Here $\alpha = 0.5$ is the deposition coefficient of H_2O molecules on ice [see *Haag et al.*, 2003], v_{th} is their thermal speed, D is their diffusion coefficient in air, v is their specific volume in ice, and n_{sat} is the H_2O vapor number density at ice saturation.

[22] Besides δ, another dimensionless parameter κ is given by

$$\kappa = \frac{2 b_1 b_2 \tau}{(1+\delta)^2}. \tag{3}$$

At $\delta \approx 1$, gas kinetic and diffusive effects on the ice particle growth rate are of similar importance. At $\kappa \approx 1$, freezing of aerosol particles and the subsequent growth of the ice particles in the formation stage occur over similar timescales.

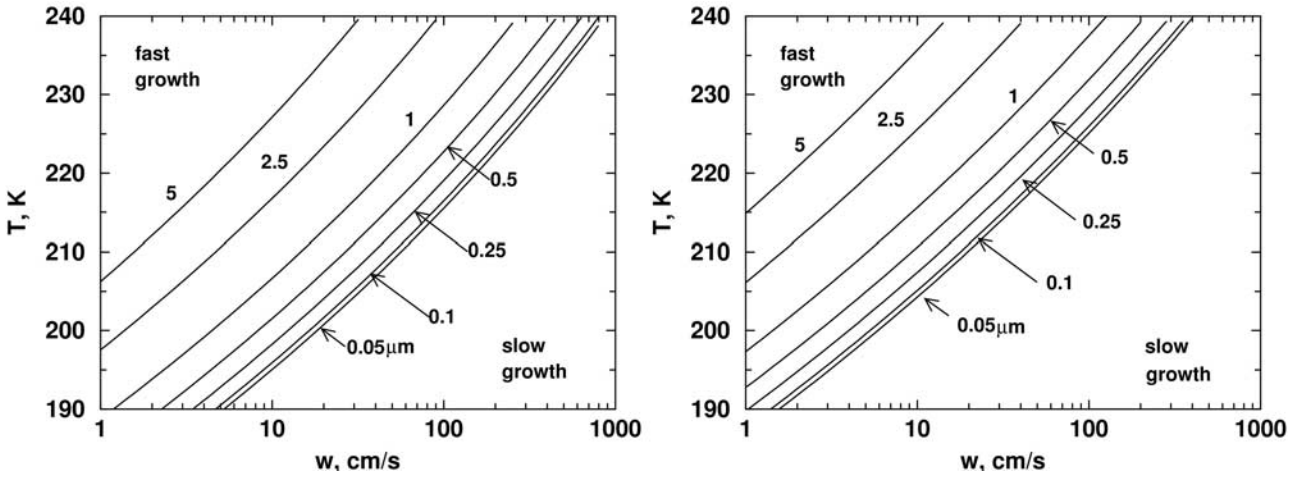

Figure 1. (left) Homogeneous freezing with $1.4 < S_{cr}(T) < 1.7$. (right) Heterogeneous freezing with a quite low freezing threshold $S_{cr} = 1.2$. The solid curves, labelled with r_0 in units of μm, connect the values of w and T (where $S_i = S_{cr}$) for which $\kappa = 1$, evaluated for an H_2O deposition coefficient on ice of 0.5. The regions above (below) each curve indicate parameter combinations $\{w, T, r_0, S_{cr}\}$, for which growth takes place in the fast (slow) growth regime. For a given radius r_0 the slow growth regime extends over a larger region in the $\{w, T\}$ space in the case of heterogeneous freezing.

[23] The timescales can be used to define two growth regimes. In the slow growth regime, valid for $\kappa < 1$, freezing occurs in a burst. All particles with different sizes freeze almost simultaneously, and details of the aerosol size distribution control vapor deposition and ice particle growth. In the fast growth regime, valid for $\kappa > 1$, freezing of new particles continues over an extended period of time, while the quickly growing ice particles lose information about their initial size.

[24] Which regime applies in a given situation is determined by the combination of w, T, r_0, and S_{cr}. In the case of homogeneous freezing the critical freezing saturation ratios S_{cr} are known and are mainly a function of T (besides a weak dependence on r_0). In the case of heterogeneous freezing, S_{cr} is regarded as a parameter that is determined by the freezing properties of the IN; see section 2.3.

[25] Figure 1 (left) shows curves along which $\kappa = 1$ for several combinations of w, T, and r_0 to distinguish both regimes for homogeneous freezing. The curves shown in Figure 1 (right) have been derived with $S_{cr} = 1.2$, for simplicity, to illustrate one specific case of heterogeneous freezing.

[26] As the supersaturation may decrease when switching from the homogeneous mode to the heterogeneous mode, the initial ice particle growth rate decreases. This implies that τ_g increases relative to τ, and κ takes on smaller values. Hence, keeping all other quantities unchanged, more cases can be attributed to the slow growth regime in the case of heterogeneous freezing. For $S_{cr} = 1$ the slow growth regime is realized for all combinations $\{w, T, r_0\}$. As a result, the resulting ice particle concentrations will be more sensitive to variations of the initial size of the freezing aerosol particles than they are in the case of homogeneous freezing, where this sensitivity is very small, as noted previously [*Kärcher and Lohmann*, 2002a].

2.1.2. Ice Particle Number Densities

[27] The number concentration of ice particles n_i, bounded by the total number of liquid particles or IN n, and the radius r_s of the smallest freezing particles follow from

$$\frac{a_1 S_{cr}}{a_2 + a_3 S_{cr}} w = \int_{r_s}^{\infty} dr_0 \frac{dn}{dr_0} R_{i,m}, \tag{4a}$$

$$n_i = \int_{r_s}^{\infty} dr_0 \frac{dn}{dr_0} \leq n, \tag{4b}$$

$$R_{i,m} = \frac{4\pi}{v} \frac{b_1}{b_2^2} \frac{\delta^2}{1+\delta} \left\{ 1 - \frac{1}{\delta^2} + \frac{1}{\delta^2} \left[\frac{(1+\delta)^2}{2} \sqrt{\kappa} + \frac{1}{\sqrt{\kappa}} \right] \right.$$

$$\left. \cdot \sqrt{\pi} e^{1/\kappa} \mathrm{erfc}\left(\frac{1}{\sqrt{\kappa}} \right) \right\}. \tag{4c}$$

The coefficients appearing in equation (4a) depend on T and on air pressure p and are determined by the adiabatic changes of the state variables and the ice particle growth law. They are defined by: $a_1 = L_s M_w g/(c_p R T^2) - Mg/(RT)$, with the molecular masses of air M and water M_w, the latent heat of sublimation L_s, the constant of gravity g, the heat capacity at constant pressure c_p, and the universal gas constant R; $a_2 = 1/n_{\mathrm{sat}}$; $a_3 = L_s^2 M_w m_w/(c_p p T M)$, with the mass of a water molecule m_w. In equation (4c) the complementary error function is defined by $\mathrm{erfc}(x) = 1 - (2/\sqrt{\pi}) \int_0^x dt\, e^{-t^2}$. Expressions for the ice particle radius and mass after freezing are also available [*Kärcher and Lohmann*, 2002b] but are not given here as they are not used in the remainder of this work.

2.1.3. Scaling Laws

[28] Scaling laws for $R_{i,m}$ and n_i as a function of w, T, and r_0, valid in both the fast and slow growth regimes, have been provided by *Kärcher and Lohmann* [2002b]. Here we focus on scaling with S_{cr}, which is not known a priori, as in

the case of homogeneous freezing. In the latter case the values

$$S_{cr}^{\mathrm{hom}} = 2.418 - T[\mathrm{K}]/245.68 \tag{5}$$

denote the threshold ice saturation ratios required to freeze one aerosol particle of radius $r_0 = 0.25$ μm within a time interval $\Delta t = 1$ s. Heterogeneous freezing thresholds S_{cr}^{het} are addressed in section 2.3. We note in passing that freezing thresholds do not depend only on the choices of particle size and time interval. For example, S_{cr} may be several percent higher when a constant cooling rate is present during freezing compared with freezing at constant temperature or when the aerosol composition is not in thermodynamic equilibrium; for a discussion of the dynamical character of S_{cr}, see *Haag et al.* [2003].

[29] Equation (5) has been derived using the activity parameterization for J_{hom} provided by *Koop et al.* [2000a]. More precisely, for fixed T we varied the water activity a_w until the product $4\pi r_0^3\, J_{\mathrm{hom}}(a_w, T)\, \Delta t/3$ equaled unity. The critical value for S_i then simply follows from $S_{cr}^{\mathrm{hom}} = a_w/a_w^{\mathrm{ice}}$, where a_w^{ice} is the water activity of the same particle in equilibrium with ice:

$$a_w^{\mathrm{ice}}(T) = \exp\left(\frac{c_1 + c_2 T + c_3/T + c_4 \ln(T)}{c_5 T}\right), \tag{6}$$

with $c_1 = 210368$, $c_2 = 131.438$, $c_3 = -3.32373 \times 10^6$, $c_4 = -41729.1$, $c_5 = 8.31441$, and T in units of K [*Koop et al.*, 2000a].

[30] The variable b_1 in equation (2) is directly proportional to the supersaturation $(S_{cr}^{\mathrm{het}} - 1)$. The saturation threshold also appears in equations (4a) and (4c) and in the parameter κ defined in equation (3). To simplify expressions, we set $a_2 > a_3 S_{cr}^{\mathrm{het}}$, which is a good approximation [*Kärcher and Lohmann*, 2002a]. (Physically, this means that the reduction of S_i caused by latent heat release during ice particle growth is small compared to the reduction of S_i caused by depositional loss of water vapor on the growing ice particles.) Given these dependencies, the scaling laws for n_i in the fast growth regime ($\kappa \gg 1$) are given by

$$n_i \propto \frac{S_{cr}^{\mathrm{het}}}{\left(S_{cr}^{\mathrm{het}} - 1\right)^{\frac{3}{2}}}. \tag{7a}$$

In the slow growth regime ($\kappa \ll 1$) we find for small particles ($\delta \ll 1$) that

$$n_i \propto \frac{S_{cr}^{\mathrm{het}}}{\left(S_{cr}^{\mathrm{het}} - 1\right)^{3}}; \tag{7b}$$

for large particles ($\delta \gg 1$) we find that

$$n_i \propto \frac{S_{cr}^{\mathrm{het}}}{S_{cr}^{\mathrm{het}} - 1}. \tag{7c}$$

The ice concentration rises with a decreasing freezing threshold because decreasing S_{cr}^{het} slows the growth rates of the new ice particles; thus more particles are allowed to freeze because the supersaturation is maintained for a longer period of time. In principle, this is similar to the effect of decreasing T (although variations in T introduce an exponential response via n_{sat}).

[31] Common to all cases is the strong rise of n_i when the particles become nearly perfect IN ($S_{cr}^{\mathrm{het}} \to 1$). The difference between equations (7b) and (7c) is caused by the strong dependence of n_i on particle size in the slow growth regime, while n_i exhibits no dependence on r_0 in the fast growth regime, as noted in section 2.1.1. (Recall that the fast growth regime is not applicable for perfect IN.)

[32] The singularity for perfect IN is not real because n_i is always bounded by the number of aerosols n available for freezing. Even if n was not a limiting factor, n_i could not grow without bounds. The singularity in the analytical model equations (4a), (4b), and (4c) in the limit $S_{cr}^{\mathrm{het}} \to 1$ is caused by setting the freezing threshold S_{cr} equal to the peak saturation ratio $\hat{S}_i$. We have shown that this is a good approximation for homogeneous freezing, where $(\hat{S}_i - S_{cr}^{\mathrm{hom}}) \ll (S_{cr}^{\mathrm{hom}} - 1)$ holds [*Kärcher and Lohmann*, 2002a]. This is no longer valid when S_{cr}^{het} approaches unity as some (albeit small) supersaturation δs_i is caused by the vertical velocity w; δs_i is larger when cooling rates are high and temperatures are low [*Haag et al.*, 2003] because low T increases τ_g. Numerical simulations show that δs_i is of the order of a few percent when perfect IN freeze. We will exploit this fact in section 3 by replacing $(S_{cr}^{\mathrm{het}} - 1)$ by $(S_{cr}^{\mathrm{het}} - 1 + \delta s_i)$ in order to obtain better fits to numerical solutions.

2.2. Heterogeneous Nucleation

2.2.1. Factors Controlling Nucleation

[33] In striking contrast to homogeneous nucleation, any theoretical description of heterogeneous freezing must face a plethora of basic problems associated with the largely unresolved physical and chemical processes at work at the surfaces of insoluble IN in the atmospheric aerosol. The nucleation of ice germs at the surface of a solid IN may be influenced by the following processes, some of which have already been mentioned in section 1.2.

[34] Surface roughness may be caused by steps, dislocations, cracks, or other morphological irregularities [*Pruppacher and Klett*, 1997]. These defects (active sites) are believed to promote nucleation, for instance, through an inverse Kelvin effect, whereby the supersaturation in concave features increases compared to a flat surface. Such effects are probably of special importance for solid microcrystals [*Zuberi et al.*, 2001] and fractal soot particles [*Garten and Head*, 1964, 1965]. Fast crystal growth rates at high supersaturations favor the generation of surface defects, which influence rates of adsorption and surface diffusion of molecules.

[35] Soot particles from various sources are known to contain organic matter and sulfate. Pure hydrocarbons or pure hydrogenated graphites do not exhibit an ice-nucleating ability. However, chemical treatment with sulfuric acid [*Wyslouzil et al.*, 1994] or with oxidizing agents (such as OH radicals) [*Kärcher et al.*, 1996] may increase the number of hydrogen-bonding groups (active sites) and enhance the wettability, which is a necessary condition for a particle to act as an efficient IN. If enough H_2O molecules coadsorb at the surface, a supercooled liquid layer can be formed, producing a mixed particle containing a solid core surrounded by a liquid shell. The formation of such coatings

may also take place at the surfaces of mineral dust or other solid airborne particles.

[36] Preactivation or preconditioning may occur when a particle once formed ice and then experiences subsaturated conditions [*Pruppacher and Klett*, 1997]. The water molecules that were bound at the surface may not fully evaporate, leaving behind active sites belonging to (approximately) the same crystal system as ice. Some active sites may survive under subsaturated conditions. If a preactivated particle experiences supersaturation again, it may nucleate ice earlier than the previously unactivated particle under otherwise similar conditions. However, when the preactivated particle is exposed to very dry conditions for a sufficiently long time, the active sites may vanish, and with them may vanish the ability to nucleate ice efficiently.

[37] Effects of preactivation may have caused, at least in part, the very different freezing thresholds of ammonium sulfate particles that were exposed to various cooling/warming cycles [*Zuberi et al.*, 2001]. Preactivation may turn aircraft exhaust soot that forms short-lived (a few seconds to minutes) contrails into effective IN. This would be an important indirect effect increasing the potential importance of aircraft on cirrus cloudiness [*Kärcher*, 2000]. (The direct effect requires that persistent contrails form which increase cirrus cloudiness.)

[38] The number of active sites caused by morphology, chemistry, or preactivation may or may not scale in proportion to the surface area per particle. This is because the integral ice-nucleating power of an ensemble of polydisperse aerosols may be controlled by only a small fraction of particles that are the most efficient IN [*Pruppacher and Klett*, 1997]. This fraction may belong to any size category so that it may not always be justified to assume that the largest IN are the first to form ice.

[39] Homogeneous freezing is a stochastic process as water molecules join the water clusters in a random fashion to eventually form stable ice germs. It is known that large variances of heterogeneous freezing temperatures may occur in mixtures of IN with different freezing properties within one sample [*Pruppacher and Klett*, 1997]. However, it may still be reasonable to assume stochastic freezing in a chemically uniform sample of pure IN, as we will do in section 2.3 in the absence of more detailed experimental information.

[40] The number of ice crystals forming in the presence of both liquid particles and IN depends on whether the different particle types are externally or internally mixed; see section 2.3.3. For an external mixture of pure particles the number and size of the particles relative to each other matters in determining the peak supersaturation achieved during freezing. For internally mixed particles, two variables may serve to describe the relative importance of homogeneous versus heterogeneous nucleation: the core number fraction (CNF), indicating how many of the liquid droplets of a given size contain a solid core; and the core volume fraction (CVF), equal to $(r_c/r_0)^3$, as a measure of the volume of the solid core (radius r_c) immersed in droplets (radius $r_0 > r_c$) relative to the droplet volume without immersion.

2.2.2. Freezing Modes

[41] Heterogeneous freezing involves several distinct modes of action [*Vali*, 1985b]. Deposition nucleation describes the formation of ice in a supersaturated vapor environment, in which ice germs nucleate at the surface of a dry solid driven by vapor deposition. Deposition nucleation may not occur frequently in the upper troposphere since the conditions required for forming dry solid particles (relative humidities below the efflorescence relative humidities of, for instance, ammonium sulfate aerosols) are probably rare [*DeMott et al.*, 1997; *Colberg et al.*, 2002]. Deposition nucleation may principally occur on the surfaces of mineral dust particles, but it seems unlikely that mineral dust particles survive their transport to the upper troposphere without acquiring a liquid coating or becoming internally mixed in liquid aerosol particles.

[42] Freezing nucleation describes the formation of ice in a supercooled liquid environment. The most important freezing modes refer to contact freezing, condensation freezing, and immersion freezing. Contact freezing involves collisions between IN and haze or water droplets. This process is inefficient owing to the low number densities of aerosol particles and to the absence of liquid water drops at the cirrus levels ($T < 235$ K). For instance, the timescale for coagulation between a particle from the accumulation mode with a mean radius of 60 nm, a total concentration of $n = 300$ cm^{-3} [*Schröder et al.*, 2002], and an IN of the same size is given by $2/(Kn) = 77$ days, with a coagulation rate $K \simeq 10^{-9}$ cm^3 s^{-1} [*Pruppacher and Klett*, 1997].

[43] During condensation freezing a cloud condensation nuclei initiates freezing during cloud droplet growth. During immersion freezing a nuclei suspended in the body of a liquid particle initiates freezing. While condensation freezing is usually defined to require water saturation prior to freezing, which rarely occurs in the upper troposphere, we are left with immersion freezing as the most important freezing mode at cirrus levels, where the IN is included in a supercooled solution droplet. We use this term for IN volume fractions low enough to ensure that at least a multilayer coating is present at the surface of the IN. If the coating makes up less than a monolayer, that is, in the limit CVF $\rightarrow$ 1, the IN tends to act in the deposition mode.

2.3. Heterogeneous Nucleation Rates and Freezing Thresholds

[44] As in the case of aerosol nucleation from the vapor phase [*Clement and Ford*, 1999], n_i does not directly depend on the nucleation rate J but is largely determined by the freezing thresholds S_{cr} and the T dependence of ln (J) [*Kärcher and Lohmann*, 2002a]. In principle, these parameters can be inferred from measurements. However, expressions for J are needed in numerical models to predict cloud formation and, in the absence of other data sources, to derive the freezing thresholds S_{cr}; compare section 2.1.3 for the homogeneous case.

[45] One way to calculate heterogeneous nucleation rates would be to reconcile the activity-based parameterization of J_{hom} with the classical homogeneous nucleation theory by fitting the surface tension and diffusion activation energy as a function of a_w, a possibility indicated by *Koop et al.* [2000a]. Using the concepts of classical heterogeneous nucleation theory [*Pruppacher and Klett*, 1997], an extension to freezing of IN would then be straightforward. However, conceptual difficulties render this strategy suspect as thermodynamic variables may depend on other parame-

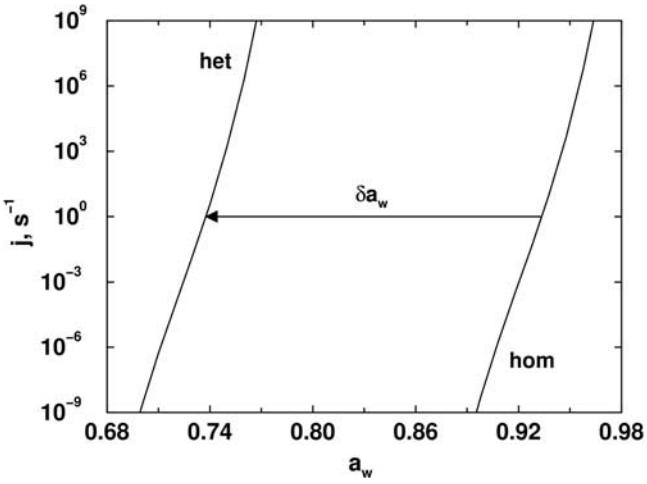

Figure 2. Nucleation rates per particle per second versus water activity at 220 K. Homogeneous (right curve) and heterogeneous (left curve) rates are separated by the amount $\delta a_w \simeq 0.2$, resulting from $S_{cr}^{\text{het}} = 1.2$. The same particle that freezes homogeneously at $a_w \simeq 0.93$ would freeze heterogeneously at $a_w \simeq 0.73$ under these conditions.

ters besides a_w, and the introduction of contact angles or misfit parameters leads to functional dependencies that may contradict observations [*Pruppacher and Klett*, 1997].

2.3.1. Pure IN Particles

[46] In this work we present a method to formulate simple expressions for J_{het} that (1) reduce to the homogeneous rates by *Koop et al.* [2000a] in the limit of pure liquid particles (as employed in our parameterization for homogeneous freezing) and that (2) are flexible enough to fit any given experimental data on S_{cr}^{het} from experiments with immersion or deposition nuclei. The values of S_{cr}^{het} may depend on any parameter (the size of the IN, the number and chemical nature of active freezing sites covering the IN surface, among other factors, denoted by the set $\{X_k\}$), determining the freezing behavior of the IN in question.

[47] In the activity parameterization, J_{hom} depends on $\Delta a_w = a_w - a_w^{\text{ice}}(T)$. (As explained previously, we identify a_w with the ambient relative humidity divided by 100 when using it in the homogeneous parameterization scheme [*Kärcher and Lohmann*, 2002a].) The thresholds of equation (5) for the freezing of one particle ($r_0 = 0.25$ μm) in 1 s are obtained for $\Delta a_w = \text{const} = 0.32$ independent of T. We now prescribe S_{cr}^{het} and search for an expression of J_{het} that is consistent with this number. To obtain J_{het}, we shift a_w by an amount δa_w such that heterogeneous freezing occurs at the prescribed value S_{cr}^{het}. The corresponding values of the unknown δa_w follow from the requirement:

$$a_w^{\text{het}} + \delta a_w - a_w^{\text{ice}} \equiv a_w^{\text{hom}} - a_w^{\text{ice}} = \text{const};$$

solving for δa_w yields

$$\delta a_w = \left[S_{cr}^{\text{hom}}(T) - S_{cr}^{\text{het}}(\{X_k\})\right] a_w^{\text{ice}}(T). \tag{8}$$

In equation (8), S_{cr}^{hom} is not allowed to exceed the liquid water saturation limit, which is given by $1/a_w^{\text{ice}}$. For our choice of S_{cr}^{hom} this occurs at temperatures >233 K. The nucleation rate is given by

$$J_{\text{het}}(a_w, T, \{X_k\}) = \Delta \cdot J_{\text{hom}}(a_w + \delta a_w, T). \tag{9}$$

The equation $4\pi r_c^2 J_{\text{het}} \Delta t = 1$ (again with $\Delta t = 1$ s and $r_0 = 0.25$ μm) returns the values S_{cr}^{het} that have been imposed to compute the activity shifts. The value $\Delta \simeq 30$ nm is the ratio of kinetic prefactors from the nucleation rates taken from the work of *Pruppacher and Klett* [1997]. (Note that the number of ice particles formed per unit time may not simply scale with the IN (core) surface area as J_{het} is allowed to depend on r_c whenever S_{cr}^{het} contains such a dependence.) We inhibit the nucleation of ice germs in equation (9) on core particles that are smaller than typical germ sizes.

[48] Figure 2 illustrates how the shifted activity method works. We have plotted the nucleation rates j per particle per unit time, evaluated for $r_c = r_0 = 0.25$ μm, $T = 220$ K, and $S_{cr}^{\text{het}} = 1.2$, as a function of the water activity. (We assume that the IN is covered by a thin coating to ensure that the immersion mode is active and deposition nucleation does not take place.) The heterogeneous rate (left curve) takes approximately the same functional form as the homogeneous rate (right curve) but is shifted by the amount δa_w. The shapes of the curves are not exactly identical because the factor Δ in equation (9) reflects different kinetic prefactors.

[49] Figure 3 depicts homogeneous and some heterogeneous freezing saturation ratios. At fixed T the differences

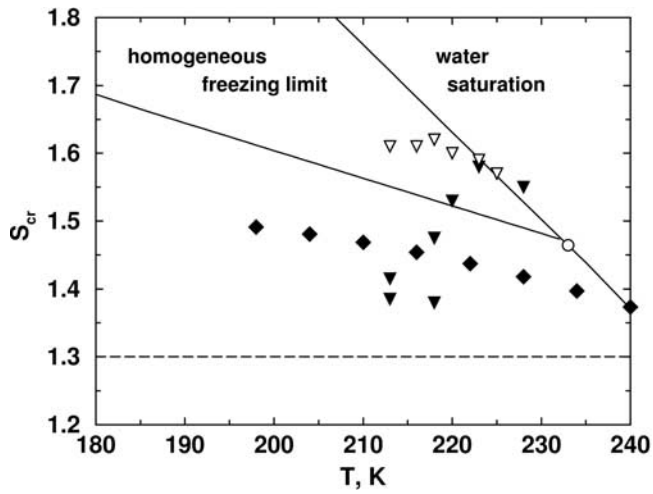

Figure 3. Freezing threshold saturation ratios over ice versus temperature for homogeneous freezing (upper left solid curve) from equation (5) and for a constant value of 1.3 (dashed curve). The upper right solid curve shows the ice saturation ratios where liquid water would be saturated. Homogeneous freezing at temperatures to the right of the open circle occurs at water saturation. Also shown are experimental data for black carbon (BC) particles from the work of *DeMott et al.* [1999] (filled/open triangles for multilayer/monolayer coverage with H_2SO_4) and for ammonium sulfate particles with mineral dust immersions from the work of *Zuberi et al.* [2002] (diamonds). The latter authors have fitted their data to a shifted water activity.

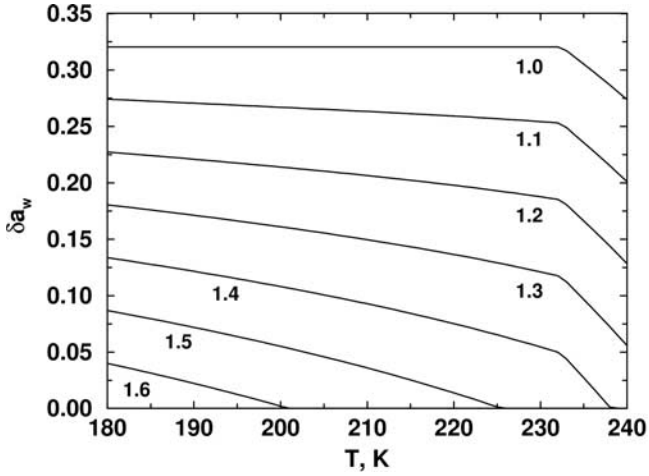

Figure 4. Shifts of the water activity as a function of temperature from equation (8) assuming constant heterogeneous freezing thresholds S_{cr}^{het}, as indicated on the curves. Values $\delta a_w = 0$ indicate that the homogeneous freezing threshold is lower than or equal to S_{cr}^{het}.

between the homogeneous limit and the various heterogeneous thresholds (for example, the constant 1.3 shown as a dashed line) determine the activity shifts of equation (8) and the nucleation rates of equation (9). The measurement data reproduced with symbols are used further in section 4. Figure 4 depicts a series of activity shifts δa_w for constant values S_{cr}^{het} in the range from unity to 1.6. The shifts are zero whenever $S_{cr}^{\text{het}} \geq S_{cr}^{\text{hom}}$. Negative values of δa_w are not allowed here because homogeneous freezing nuclei are always available in the atmosphere.

[50] The homogeneous water activity criterion, and hence equation (5), is applicable to freezing of ice in liquid polar stratospheric clouds composed of supercooled ternary solutions. The corresponding freezing temperatures in the winter polar stratosphere are near 188 K. Equation (9) may also be applied under these low temperature conditions. The extrapolation to 180 K, however, should be taken with care.

[51] Our proposed shifted activity method is clearly empirical as it has not been derived from first principles. Not all aspects of heterogeneous nucleation are, possibly, predicted by equation (9). From our assumptions it follows that

$$\partial \ln(J_{\text{het}})/\partial T = \partial \ln(J_{\text{hom}})/\partial T,$$

while the true dependence, and thus the timescale τ, may be different from equation (1). In the absence of experimental information it is plausible to use the homogeneous expression until contradicted by measurements. Alternatively, we could multiply it with the constant c in equation (1) and use the product as one single-fit parameter. In any case, as the main effect of heterogeneous nucleation is to lower the freezing relative humidities, we argue that the shifted activity method is a very flexible tool to account for this effect.

2.3.2. Mixed Particles

[52] One physically reasonable way to define a nucleation rate j_{mix} for mixed particles suited for implementation in numerical models is given by

$$j_{\text{mix}} = A_c J_{\text{het}} + (1 - \text{CVF}) V_0 J_{\text{hom}}, \tag{10}$$

where $A_c = 4\pi r_c^2$, $V_0 = 4\pi r_0^3/3$, and $\text{CVF} = (r_c/r_0)^3 < 1$. (The symbol j denotes a true rate, indicating the number of ice germs formed per unit time.) This expression describes combined homogeneous freezing within a spherical shell of liquid surrounding an IN and heterogeneous freezing taking place at the surface of the IN. In constructing equation (10) we assume that heterogeneous and homogeneous modes act independently in the mixed particle.

[53] The mixed particle may contain immersions of different chemical types, for example, BC and dust. While there are no robust data available to test under which circumstances equation (10), which is based on one chemically uniform type of IN, yields an accurate description of the freezing kinetics, the situation is even worse in this case, for which reason we do not work it out in more detail. At this point it is sufficient to note that it may be reasonable to assume some concentration-based average of the freezing rates of single-component IN from equation (9) to compute the freezing rates for more complex mixed particles with several IN types. Besides being a function of T, j_{mix} now depends on r_c and CVF. A possible dependence on CNF will be considered next.

2.3.3. Internal Versus External Mixtures

[54] So far, we have focused on a single aerosol particle type. The atmospheric aerosol may be composed of mixtures of different particle types. As the mean age of upper tropospheric aerosols is rather large, especially in the Southern Hemisphere, where anthropogenic sources are often absent [*Clarke and Kapustin*, 2002; *Minikin et al.*, 2003], one may expect most aerosol particles to be internally mixed. In the Northern Hemisphere, direct emissions of particles by aircraft or after rapid transport of pollutants from the continental boundary layer (in particular in deep convection in the tropics) may cause particles from different sources to stay externally mixed for many days or weeks as the timescale for coagulation (the process transforming external to internal mixtures) is rather long due, primarily, to the low particle concentrations in the upper troposphere.

[55] To describe this situation in our framework, a logical extension of equation (10) might be given by equations (11a) and (11b):

$$j_1 = \left(1 - \sum_k \text{CNF}_k\right) V_0 J_{\text{hom}}, \tag{11a}$$

$$j_{2,k} = \text{CNF}_k j_{\text{mix,k}}, \tag{11b}$$

with $\text{CNF}_k < 1$. The term j_1 describes homogeneous freezing of aerosol particles without immersions. The term $j_{2,k}$ is the mixed particle contribution. The parameter CVF in j_{mix} now contains a subscript k to denote the IN type. In applying equations (11a) and (11b), one must take care that the number of ice particles formed from type k particles is limited by n_k. The total number n_i cannot exceed the sum of n_k over all IN types; the number densities n_k must be split up into n_1 particles freezing homogeneously and $n_{2,k}$ particles freezing heterogeneously. We underline that the number of ice crystals formed when using $j_k = j_1 + j_{2,k}$ depends on w as low vertical velocities may only activate the heterogeneous mode, but most of the particles may nucleate homogeneously in a vigorous updraft under otherwise unchanged

conditions [*DeMott et al.*, 1997; *Jensen and Toon*, 1997; *Sassen and Benson*, 2000].

[56] A separate parameterization for the freezing of different particle types and their competition for the available water vapor is required when the combined homogeneous/heterogeneous parameterization is coupled to a model that resolves different types of particles. This task is beyond the scope of the present paper but will be addressed in future work. However, we relate the competition between multiple particle types to the Twomey effect in cirrus clouds in section 4.2.

2.3.4. Immersion Versus Deposition Freezing

[57] When a pure particle freezes homogeneously, it is usually a good approximation to assume that nucleation of one ice germ in the solution causes rapid (within seconds or faster) freezing of the whole liquid [e.g., *Pruppacher and Klett*, 1997; T. Koop, personal communication, 2002], the ice germ growth rate depending on the solute concentration and the freezing temperature. We implicitly make the same assumption in the case of a mixed particle, irrespective of whether nucleation is triggered by the IN surface or by the liquid volume surrounding the inclusion. The initial radius of the freshly produced ice particle is then equal to the radius r_0 of the freezing aerosol particle.

[58] However, this may be different when initially dry IN freeze in the deposition mode. In one extreme case where nucleation is slow, only a few or even only one single critical germ forms at the IN surface, and the initial radius of the ice particle approaches the size of the ice germ (typically a few nanometers). If nucleation occurs rapidly, the whole IN surface may quickly be covered with supercritical germs before substantial depositional growth takes place, and the initial size of the IN may be a better measure for the crystal size.

[59] This effect modifies the growth rates and vapor depletion timescale of equation (2) and thus the number of ice particles predicted by our parameterization. This point should be borne in mind when applying the theoretical framework to deposition nuclei, which is beyond the scope of this work. (Recall that deposition nuclei are probably scarce in the upper troposphere.)

2.3.5. Monodisperse Versus Polydisperse Particles

[60] If the mixed aerosol is polydisperse, CNF and CVF must be defined over a continuous range of particle sizes. However, experimental data for heterogeneous freezing of IN to validate both numerical simulations and the parameterization are very scarce and are mostly insufficient to aid in deciding which particles from the ensemble were responsible for the observed ice formation. Also, as mentioned in section 2.2.1, the largest IN may not be the ones that freeze first.

[61] In equations (4a) and (4b) we assume that ice crystals first nucleate in the largest aerosol particles, just as for homogeneous freezing. In the latter case this is a reasonable assumption; although there is some finite probability to nucleate ice also in small particles, this probability is small due to the Kelvin effect, which reduces the water activity in small aerosol particles. In the case of heterogeneous nucleation the situation may be more difficult, as discussed in section 2.2.1, and the assumption $j_{het} \propto A_c$ may become invalid. In such a situation we have two alternatives. First, we could multiply the integrands in equations (4a) and (4b) with some prescribed function that describes the fraction of IN that nucleate at a given size. However, such information is generally not available.

[62] Alternatively, it is possible to fit the parameterization in a monodisperse approximation to freezing measurements employing size-distributed aerosols by using the radius r_0 of the freezing particle as a fit parameter. In the absence of any knowledge on the freezing aerosol fraction, r_0 can be set equal to the median number radius; otherwise, r_0 can be fixed if the size of the freezing particles is approximately known.

2.4. Summary

[63] We summarize some important points that emerged from the discussion in sections 2.1–2.3. Parameterizing heterogeneous freezing is much more difficult than it is for homogeneous freezing because the factors controlling heterogeneous processes are not well known, both experimentally and theoretically. In this situation we are satisfied if we can find at least an empirical description for the heterogeneous nucleation rate that includes the homogeneous case as a limit and can be adjusted to available freezing data.

[64] We have proposed the shifted activity parameterization in conjunction with the homogeneous activity rate model to reach this goal. The shifted activity method is flexible as it can account for the fact that the heterogeneous freezing thresholds needed to determine the nucleation rates are allowed to depend on parameters such as vertical velocity, temperature and size, and number and volume fraction of IN within liquid aerosol particles, among other factors. It may, however, not reproduce all details of the real nucleation event.

[65] Uncertainties are introduced by (1) the mixed nature of most aerosol particles in the upper troposphere; (2) the presence of more than one chemically distinct type of IN in mixed aerosols; (3) the possible presence of external mixtures near source regions (convection, aircraft, in situ nucleation), giving rise to a competition between heterogeneous and homogeneous freezing modes; (4) the lack of data to constrain the size dependence of ice formation in polydisperse IN; (5) the growth kinetics of ice forming in thin and submonolayer coatings; and (6) the timescale for the freezing event that may not only depend on the cooling rate.

3. Results and Discussion

[66] We consider immersion freezing of one type of chemically uniform particle. When applying equation (4a), recall that we are left with two fit parameters: the freezing timescale τ via the constant c and/or $\partial \ln(J)/\partial T$ and the excess supersaturation δs_i.

3.1. Numerical Simulations

[67] The numerical parcel model Advanced Particle Simulation Code (APSC) employed here has been developed at the Deutsches Zentrum für Luft- und Raumfahrt and is described in more detail by *Lin et al.* [2002] and *Haag et al.* [2003]. It has also been employed for the validation of the homogeneous parameterization [*Kärcher and Lohmann*, 2002a, 2002b]. As we will use the same model setup as in these four studies, the APSC is not described further here.

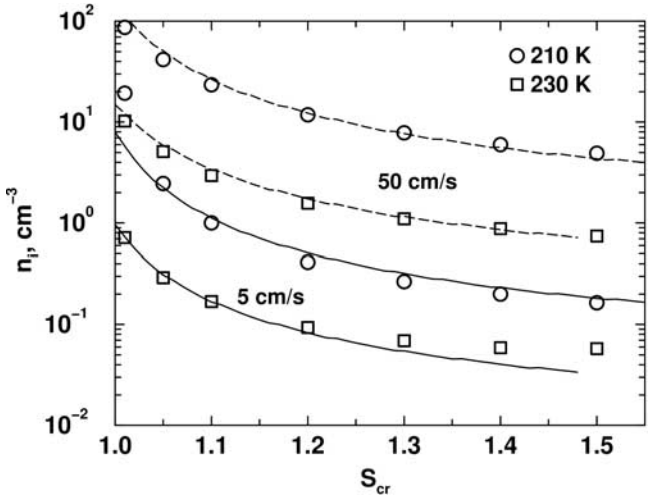

Figure 5. Peak ice particle number densities versus freezing saturation ratios for two different initial temperatures (ice saturation) and vertical velocities. Symbols (curves) indicate results from numerical simulations (parameterizations) for immersion freezing in the limit of a thin coating (CVF = 0.99). The solid curves have been obtained with $c = 60$, $\delta s_i = 0.05$ (230 K) and $c = 40$, $\delta s_i = 0.01$ (210 K); the dashed curves have been obtained with $c = 20$, $\delta s_i = 0.07$ (230 K) and $c = 12$, $\delta s_i = 0.07$ (210 K).

[68] The water activity is a well-characterized quantity in the liquid volume fraction of mixed particles, and the IN volume fractions CVF follow from the prescribed size distributions of the liquid and IN components in the aerosol particles. While we identify a_w with the ambient relative humidity in the parameterization scheme, we calculate water activity in the liquid as a function of particle composition and do not invoke any equilibrium assumptions in APSC. The simulations further take into account the Kelvin effect in the growth equations for small aerosol particles and ice crystals.

3.2. Thin Coatings

[69] We start the comparison between analytical and numerical models with IN that are covered by a thin coating of liquid (CVF = 0.99, independent of the size). For instance, an IN with $r_c = 0.3$ μm covered by a coating of 1 nm results in the above value for CVF. In the APSC and in the parameterization we assume a lognormal IN distribution with a mean number radius of 0.032 μm, a geometric standard deviation of 1.6, and a total number concentration of $n = 300$ cm^{-3}. (All particles, dry H_2SO_4, IN, and wetted with H_2O, are assumed to be spherical.) Note that n likely exceeds atmospheric concentrations of IN by orders of magnitude and has been chosen such that n does not limit the number of ice particles formed.

[70] Figure 5 depicts the peak ice number concentrations (the maximum number densities of ice particles formed in the rising air parcel) as a function of the IN freezing saturation ratios for vertical velocities of 5 cm s^{-1} (solid curves) and 50 cm s^{-1} (dashed curves) and for temperatures of 210 K and 230 K, as indicated in the legend. The symbols represent APSC results; the curves result from solving equation (4a) using various combinations of the free parameters c and δs_i.

[71] The dependence of n_i on S_{cr}^{het} agrees with the theoretical expectations summarized in section 2.1.3. The number of crystals formed increases considerably (by more than an order of magnitude) when going from the homogeneous limit to $S_{cr} = 1.01$. (The homogeneous limits are represented by the rightmost symbols in Figure 5.) However, n_i begins to rise significantly only when S_{cr} falls below ~1.3 or so. In contrast to pure homogeneous freezing, we obtain reasonable fits only when we vary the free parameters between runs with different T or w, which requires more careful adjustment of the parameterization with the help of a numerical model prior to applications.

[72] All runs start at ice saturation, implying that the lower freezing temperatures are, the higher is S_{cr}^{het} because of the constant cooling rate. Initializing all runs at the respective freezing thresholds would slightly lift the curves and symbols (almost invisible when $S_{cr}^{\text{het}} < 1.1$ and by 20% at most near the homogeneous thresholds) but would not change the behavior of n_i as a function of S_{cr} as shown in Figure 5. We note that the values of n_i do not necessarily change smoothly when increasing CVF from 0.99 to unity as the freezing modes may switch from immersion to deposition freezing when the liquid coverage approaches a monolayer at the IN surface; see section 2.3.4.

3.3. Variable IN Volume Fractions

[73] Figure 6 depicts the effective freezing thresholds of mixed particles (curves) as a function of the IN volume fraction CVF derived using equation (10) along with the requirement $j = 1$ s^{-1}. Each curve is labelled with a heterogeneous freezing threshold S_{cr}^{het} used to calculate J_{het}. We have prescribed $r_0 = 0.25$ μm and varied r_c according to $r_c = \text{CVF}^{1/3} r_0$. The freezing temperature was 220 K in all cases.

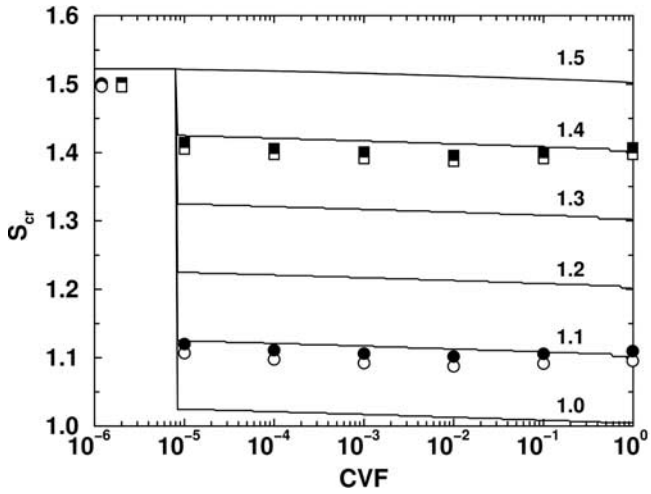

Figure 6. Effective freezing saturation ratios of mixed particles versus the volume fraction of the immersed IN at 220 K. The label on each curve denotes the prescribed heterogeneous freezing threshold S_{cr}^{het} used to calculate the heterogeneous contribution to the overall nucleation rate of equation (10). Heterogeneous freezing is inhibited for IN sizes smaller than the size of an ice germ, corresponding to CVF $\leq 8 \times 10^{-6}$. The symbols represent results from numerical simulations. See text for details.

[74] When r_c falls below the size of an ice germ (here approximated as 5 nm), we inhibit heterogeneous freezing and set $J_{het} = 0$. As a result, we obtain the homogeneous freezing threshold 1.52 at the lowest volume fractions (CVF $\leq$ CVF$_*$ = (5 [nm]/r_0)^3 = 8 $\times$ 10^{-6}). At CVF = 0.99 we obtain S_{cr}^{het}. In between these limits the effective freezing thresholds stay nearly constant and are only slightly higher than the heterogeneous values. Similar results are obtained for other values of T and r_0.

[75] This characteristic behavior of S_{cr} is brought about by the strong rise of $A_c J_{het}$ when S_i becomes larger than S_{cr}^{het} so that $A_c J_{het} \gg (1 - CVF)\, V_0 J_{hom}$ even for small values of CVF. The slight increase of S_{cr} with falling CVF above CVF$_*$ is caused by decreasing values of r_c. Both contributions to the overall nucleation rate j_{mix} become equally important only when homogeneous and heterogeneous freezing thresholds are comparable.

[76] The symbols in Figure 6 are APSC results for two representative cases, S_{cr}^{het} = 1.1 (circles) and 1.4 (squares). The updraft speed was 5 cm s^{-1}, the initial temperature was 223 K, and the initial aerosol number density was 300 cm^{-3}. The geometric standard deviation and mean mass radius of the H_2SO_4 and the IN distribution was 1.6 and 0.055 μm, respectively. The total masses of H_2SO_4 and IN were varied to yield the size-independent CVF values that can be read off from the positions of the symbols in Figure 6.

[77] The open symbols depict the ice saturation ratios at the time when 5 $\times$ 10^{-3} ice particles formed per cm^3 of air. These values define the freezing thresholds. The solid symbols depict the peak ice saturation ratios typically achieved somewhat later, when most of the ice particles have nucleated. Pairs of points for the same CVF and S_{cr}^{het} lie close together, which is expected for the moderate updraft speed. They slightly decrease from CVF = 0.99 − 0.01 but then follow the slight upward trend down to lower values. The agreement with the curves is not perfect because the simulations assume a polydisperse aerosol with variable wet particle radii r_0 (changes of r_0 are most pronounced for CVF > 0.01), while the analytic model assumes monodisperse particles with fixed r_0. Additionally, the requirement j = 1 s^{-1}, used to compute the curves in Figure 6, is probably too stringent compared to the simulations.

[78] What do we learn from this comparison? In our approach to calculate mixed particle freezing rates the volume fraction of IN immersed in liquid particles is not an important factor in determining the freezing thresholds of the mixed particles. While its impact on S_{cr} is small, the parameter CVF indicates when the freezing mode switches from heterogeneous to homogeneous freezing at its approximate lower limit CVF$_*$. The transition region near CVF$_*$ is very sharp for monodisperse IN and broadens for polydisperse particles. The relative insensitivity of S_{cr} with CVF above CVF$_*$ is a very convenient feature with regard to applications of the parameterization in numerical models. However, we recommend that one tests this feature in future laboratory studies of immersion freezing.

4. Atmospheric Implications

4.1. Contrasting Different Freezing Pathways

[79] Figure 7 depicts the probability distribution $P(n_i)$ of ice particle number density, calculated with the parameterizations. We investigate four different particle types: pure liquid particles, ammonium sulfates with mineral dust inclusions, black carbon with a multilayer coating of sulfuric acid, and a hypothetical particle with a constant freezing threshold of 1.3. The freezing thresholds, except for the latter particle type, are temperature dependent, as given in Figure 3. In using this information we presume that the laboratory results for these types of IN hold under atmospheric conditions and can be applied to the size distribution stated below; this size distribution differs from the particle sizes used during the experiments and needs further confirmation by measurements.

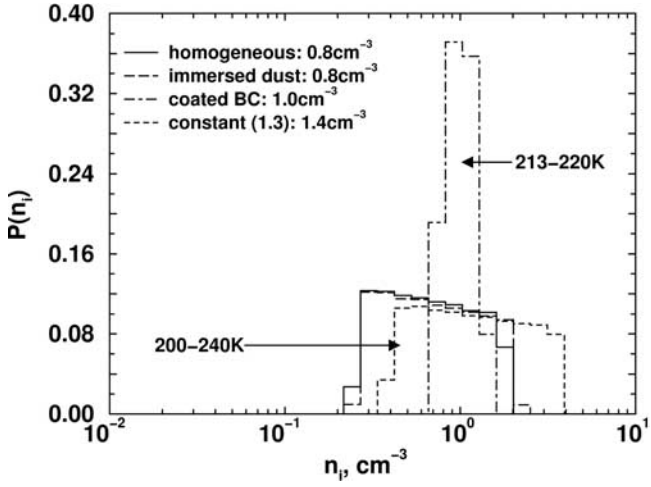

Figure 7. Probability distributions of ice particle number density for freezing of pure liquid particles (solid stair steps), mineral dust immersed in ammonium sulfates (dashed stair step), BC coated with multilayer sulfuric acid (dash-dotted stair step), and an IN with a constant freezing threshold of 1.3 (dotted stair step). The underlying temperature distribution was uniform within the ranges of validity of the laboratory measurements, as indicated. The legend displays average ice particle concentrations for each particle type. Size distribution parameters and the updraft speed were kept fixed; see text.

[80] The freezing particle size distribution used in all cases was lognormal, with n = 300 cm^{-3}, D = 0.1 μm, and σ = 1.6. The vertical velocity was w = 20 cm s^{-1}, a typical mean value observed in midlatitude cirrus [*Ström et al.*, 1997]. (The general results discussed below are similar for other choices of w.) The temperatures were generated with a random number generator, producing a uniform temperature distribution within the range 200–240 K, except for black carbon, where the range was smaller at 213–220 K, ensuring that we do not evaluate cases unsupported by the underlying measurements. Thus, also, the freezing thresholds varied, except in the case where S_{cr}^{het} = 1.3. We have used δs_i = 0.05 and c = 50, the latter in both homogeneous and heteroegneous calculations, to enable a direct comparison. The choice of δs_i has little influence on the results from the heterogeneous runs as the values of S_{cr}^{het} are well above unity. We have used 20,000 different temperatures to produce each distribution.

[81] Figure 7 gives an indication of the spread of n_i induced by the variability of T. Note that in the atmosphere,

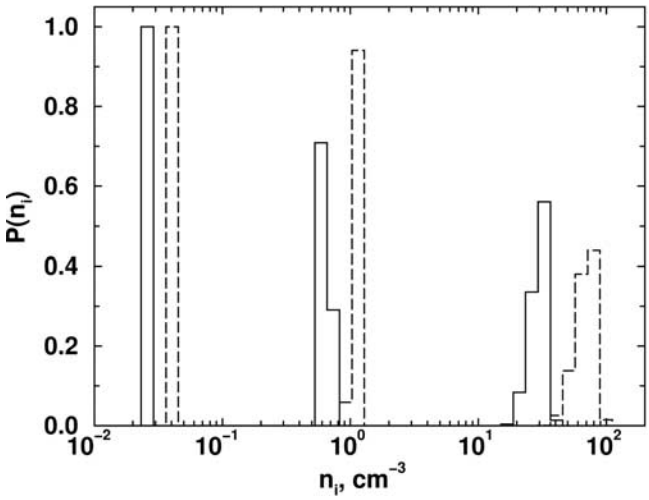

Figure 8. Probability distributions of ice particle number density for homogeneous (solid stair steps) or heterogeneous freezing (dashed stair steps). The heterogeneous freezing threshold was 1.3. Each pair of distributions was calculated at 20 cm s^{-1}, 220 K (middle); 5 cm s^{-1}, 230 K (left); and 80 cm s^{-1}, 210 K (right). Aerosol parameters were varied randomly; see text for details.

not every temperature between 200 K and 240 K is found with equal probability, as assumed here. Typically, T will vary around some mean value, creating narrower spectra $P(n_i)$. The spread of $P(n_i)$ and the mean number density of ice crystals seen in the BC results is smaller than in the other cases because the range of T used in the BC calculations is narrower than in the other cases.

[82] The differences in $P(n_i)$ between pure homogeneous freezing and the freezing of sulfates with dust inclusions are almost negligible. The results also reveal that the differences between homogeneous freezing and heterogeneous freezing of BC and dust are not very pronounced, as seen by the similar mean ice crystal concentrations given in the legend. Only when the freezing threshold takes a value of (or below) 1.3 do the distributions shift more significantly to the right (leading to a two-fold increase of the mean concentration). This finding is consistent with the results shown in Figure 5 but demonstrated here for a larger range of possible T and for IN species that could be regarded as potentially relevant to cirrus formation.

4.2. Twomey Effect for Cirrus Clouds

[83] On the basis of parcel simulations and on the parameterization for homogeneous freezing, *Kärcher and Lohmann* [2002b] concluded that the Twomey effect for cirrus clouds, that is, changes of the number of ice crystals induced by changes in the number (and size) of freezing aerosol particles, is much weaker in cirrus than in liquid water clouds and that the correlation between aerosol and ice crystal concentrations can be both positive and negative. In this section we show that the same holds for heterogeneous freezing of one type of aerosol particle.

[84] Figure 8 depicts the probability distribution $P(n_i)$ of n_i for homogeneous (solid stair steps) and heterogeneous (dashed stair steps) freezing events. The left, middle, and right distributions have been calculated with the help of our parameterization schemes for combinations (w [cm/s],T [K]) of (5,230), (20,220), and (80,210), respectively. The influence of aerosol size effects on n_i increases from left to right in Figure 8 because the vertical wind speed increases from 5 to 80 cm s^{-1} at 210 ± 10 K, leading from the fast growth regime to the slow growth regime, as shown in Figure 1.

[85] The size distributions of the freezing aerosol are characterized by the same baseline values used in section 4.1 and Figure 7, with the heterogeneous freezing threshold at 1.3. To produce the $P(n_i)$, spectral values have been varied within the ranges $\{0.5n, 1.5n\}$, $\{0.5D, 1.5D\}$, and $\{0.8\sigma, 1.25\sigma\}$, using 50,000 randomly distributed parameter combinations.

[86] Figure 8 (solid distributions) confirms the weak Twomey effect for homogeneously generated cirrus as the rather large changes of the liquid aerosol spectral parameters produce only a narrow spectrum of crystal number densities. The spectra broaden when going from the fast to the slow growth regime, as expected. Figure 8 (dashed distributions) demonstrates that the same holds for heterogeneously generated cirrus, with a slightly stronger Twomey effect only visible in the slow growth regime where aerosol size effects are most influential. Decreasing the freezing threshold S_{cr}^{het} to <1.3 would increase the Twomey effect in all cases.

[87] We emphasize that the Twomey effect in the presence of multiple particle types with different freezing thresholds requires further study. In this case the term Twomey effect refers to changes of n_i induced by adding IN to liquid aerosols; this should be a reliable scenario, at least under unpolluted upper tropospheric background conditions. In Figure 9 we show results of APSC simulations carried out with one liquid aerosol mode (S_{cr}^{hom} = 1.52) and

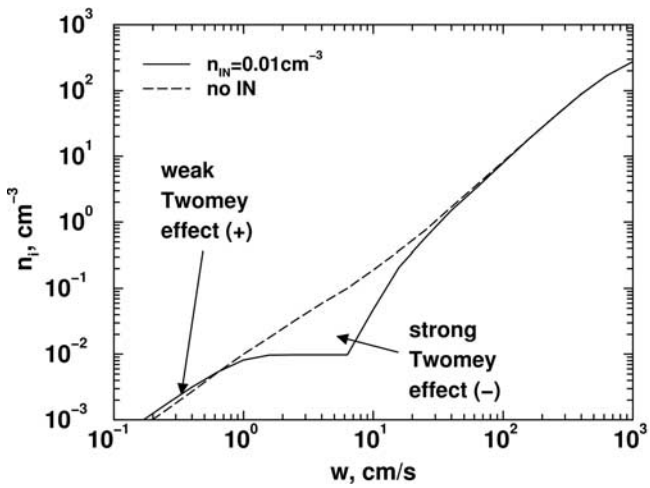

Figure 9. Number density of ice particles versus vertical velocity from APSC simulations starting at 225 K and ice saturation. In the model, 400 cm^{-3} homogeneous nuclei are present with 0.01 cm^{-3} (solid curve) and without (dashed curve) heterogeneous IN with S_{cr}^{het} = 1.3. The region where the Twomey effect is most pronounced shifts to the right (left) when the number of IN increases (decreases) or when the heterogeneous freezing threshold decreases (increases).

one IN mode ($S_{cr}^{het} = 1.3$). The initial temperature was 225 K at ice saturation. The number of IN was 0.01 cm^{-3} (solid curve) and 0 cm^{-3} (dashed curve); the number of homogeneous nuclei was 400 cm^{-3} in both cases.

[88] With increasing w, n_i increases until all available IN freeze (solid curve). For $w > 2$ cm s^{-1}, n_i remains constant because the number of ice particles formed is sufficiently high to prevent the supersaturation from further increasing. However, above a threshold vertical velocity of $\sim$6 cm s^{-1} the vapor depletion rate of existing ice particles becomes too small compared to the rate of increase of S_i rising $\propto w$, and the homogeneous mode is activated. Above 2 cm s^{-1} the number of ice crystals formed homogeneously in the presence of IN is smaller than without IN (see the dashed curve of Figure 9 for pure homogeneous freezing) because ice crystals that have formed on the IN compete for the available H_2O during the freezing event. This effect weakens as w rises and becomes unimportant for $w > 30$ cm s^{-1}. At the highest updraft speeds considered, almost all available homogeneous nuclei contribute to the formation of ice.

[89] It is clear that the number of ice crystals formed at a given combination of w and T now crucially depends on the presence of IN. In the case shown in Figure 9 we observe two regions exhibiting a Twomey effect. In the first region for $w < 1$ cm s^{-1} a rather weak, positive change of n_i is caused by adding IN and the associated decrease of the freezing threshold from 1.52 to 1.3; compare the discussions of Figures 5 and 8. In contrast, in the second region for w between 2 and 10 cm s^{-1}, that is, in synoptic-scale updrafts or in updrafts generated by weak turbulence or gravity waves, the Twomey effect becomes negative and is very pronounced. At $w = 6$ cm s^{-1}, n_i is lowered by a factor of 10 when IN are added; it is very unlikely that such a change of n_i can be induced by changes of the size distribution parameters or of the freezing thresholds of the IN alone. No Twomey effect occurs for $w > 30$ cm s^{-1} as the number of IN in this calculation is limited to 0.01 cm^{-3}. Note that this IN concentration is not an unrealistic value; compare section 1.2.

[90] Increasing or decreasing the total number of IN shifts the intermediate region where n_i levels off to higher or lower vertical velocities. The same effect is obtained when S_{cr}^{het} decreases or increases. If both freezing thresholds are similar, the Twomey effect vanishes. The quantitative results depend on T, but the numbers are not very different from those shown in Figure 9 when reducing T to 215 K. These findings are in qualitative agreement with other numerical simulations of the Twomey effect of cirrus clouds for homogeneous versus heterogeneous freezing [*DeMott et al.*, 1997; *Jensen and Toon*, 1997]. This is noteworthy as these authors investigate this issue with numerical formulations of the heterogeneous nucleation process different from the shifted activity approach developed in section 2.3.

[91] In summary, whether or not an indirect aerosol effect on cirrus clouds is actually discernable will crucially depend on the spectrum of vertical velocities active during the formation of the cirrus clouds, the concentrations of IN added to liquid background aerosols, and their freezing thresholds relative to the homogeneous limits. If the background particles themselves are composed of heterogeneous IN and freeze more efficiently than liquid nuclei, the situation becomes even more complicated.

5. Summary and Outlook

[92] We developed a physically based description of heterogeneous freezing to parameterize cirrus cloud formation by this process. Owing to the complexity of heterogeneous freezing modes, we restricted ourselves to a description of immersion freezing of one chemically uniform type of ice nuclei. We consider immersion freezing as the most likely heterogeneous freezing path in cirrus conditions as deposition nuclei are probably rare and contact freezing requires supercooled water drops to become important. We proposed the shifted activity method to compute heterogeneous freezing rates for use in numerical studies. The main results of our study are summarized as follows.

[93] 1. In particles containing ice nuclei as a core surrounded by a shell of liquid the core volume fraction is not an important factor in determining the freezing threshold of the mixed particles. However, this parameter indicates at which minimum size of the immersed particle the freezing mode switches from heterogeneous to homogeneous freezing.

[94] 2. For given updraft speeds, temperatures, and aerosol size distribution parameters, the number of ice crystals formed increases considerably (by one to two orders of magnitude) when going from the homogeneous freezing limit to a freezing threshold near ice saturation. Thus if perfect ice nuclei were present in the upper troposphere, almost all of them would form ice near ice saturation, even in slow updrafts.

[95] 3. Cirrus cloud properties are not very susceptible to changes in the properties of ice nuclei with freezing threshold saturation ratios > 1.3–1.4. This holds under the assumption that only one such type of ice nuclei is present in the freezing aerosol. The number of ice crystals formed this way is higher compared to purely homogeneous ice formation, but the differences remain within a factor of two or so (weak positive Twomey effect).

[96] 4. The Twomey effect in cirrus clouds, and thus possible anthropogenic modifications of cirrus cloud formation, can become very significant in the case of the freezing of several particle types with distinct freezing thresholds. The number of ice crystals formed in such cases is lower compared to purely homogeneous ice formation and is critically determined by the vertical velocity driving the nucleation and the number and freezing thresholds of ice nuclei relative to the liquid background particles (strong negative Twomey effect).

[97] Thus it is of paramount importance in future studies of the indirect aerosol effect on cirrus clouds to (1) allow for competition between multiple particle types in the parameterization of cirrus formation and to (2) obtain better information on the spectrum of updrafts active during cirrus formation and on the freezing properties of potential ice nuclei.

Notation

a_w water activity.
a_w^{ice} water activity at ice equilibrium.

A_c surface area of a solid IN core immersed in a droplet.
c fit parameter.
j nucleation rate per unit time per particle.
J nucleation rate coefficient for a pure particle.
n total number density of aerosol particles.
n_i total number density of ice particles.
n_{sat} saturation vapor number density over ice.
r_c radius of a solid IN core immersed in a droplet.
r_0 ice particle radius at time t_0.
$R_{i,m}$ monodisperse freezing/growth integral.
S_i saturation ratio over a flat ice surface.
s_i peak saturation ratio.
S_{cr} freezing threshold saturation ratio.
t time.
t_0 time when freezing commences.
T temperature.
w vertical velocity.
δ dimensionless parameter.
δa_w shift of water activity caused by IN.
δs_i minimum ice supersaturation for perfect IN.
κ dimensionless parameter.
τ freezing timescale.
τ_g initial growth timescale of ice particles.

[98] **Acknowledgments.** We are grateful to Thomas Koop, Paul DeMott, and Bilal Zuberi for helpful comments on a draft version of this manuscript. This research was performed within the European project "Particles in the Upper Troposphere and Lower Stratosphere and Their Role in the Climate System" (PARTS) and was supported by the National Science and Engineering Research Council of Canada and by the Helmholtz Gemeinschaft Deutscher Forschungszentren (HGF) through the project "Particles and Cirrus Clouds" (PAZI).

References

Chen, Y., S. M. Kreidenweis, L. M. McInnes, D. C. Rogers, and P. J. DeMott, Single particle analysis of ice nucleating aerosols in the upper troposphere and lower stratosphere, *Geophys. Res. Lett.*, *25*, 1391–1394, 1998.

Clarke, A. D., and V. N. Kapustin, A Pacific aerosol survey. part I: A decade of data on particle production, transport, evolution, and mixing in the troposphere, *J. Atmos. Sci.*, *59*, 363–382, 2002.

Clement, C. F., and I. J. Ford, Gas-to-particle conversion in the atmosphere: II. Analytical models of nucleation bursts, *Atmos. Environ*, *33*, 489–499, 1999.

Colberg, C., B. P. Luo, H. Wernli, T. Koop, and T. Peter, A novel model to predict the physical state of atmospheric $H_2SO_4/NH_3/H_2O$ aerosol particles, *Atmos. Chem. Phys. Discuss.*, *2*, 2449–2487, 2002.

Cooke, W. F., and J. J. N. Wilson, A global black carbon aerosol model, *J. Geophys. Res.*, *101*, 19,395–19,409, 1996.

Cotton, W. R., G. J. Tripoli, R. M. Rauber, and E. A. Mulvihill, Numerical simulations of the effects of varying ice crystal nucleation rates and aggregation processes on orographic snowfall, *J. Clim. Appl. Meteorol.*, *25*, 1658–1680, 1986.

DeMott, P. J., Laboratory studies of cirrus cloud processes, in *Cirrus*, edited by D. K. Lynch et al., pp. 102–135, Oxford Univ. Press, New York, 2002.

DeMott, P. J., D. C. Rogers, and S. M. Kreidenweis, The susceptibility of ice formation in upper tropospheric clouds to insoluble aerosol components, *J. Geophys. Res.*, *102*, 19,575–19,584, 1997.

DeMott, P. J., D. C. Rogers, S. M. Kreidenweis, Y. Chen, C. H. Twohy, D. Baumgardner, A. J. Heymsfield, and K. R. Chan, The role of heterogeneous freezing nucleation in upper tropospheric clouds: Inferences from SUCCESS, *Geophys. Res. Lett.*, *25*, 1387–1390, 1998.

DeMott, P. J., Y. Chen, S. M. Kreidenweis, D. C. Rogers, and D. E. Sherman, Ice formation by black carbon particles, *Geophys. Res. Lett.*, *26*, 2429–2432, 1999.

Diehl, K., C. Quick, S. Matthias-Maser, S. K. Mitra, and R. Jaenicke, The ice-nucleating ability of pollen, part I: Laboratory studies in deposition and condensation freezing modes, *Atmos. Res.*, *58*, 75–87, 2001.

Field, P. R., et al., Ice nucleation in orographic wave clouds: Measurements made during INTACC, *Q. J. R. Meteorol. Soc.*, *127*, 1493–1512, 2001.

Fletcher, N. H., *The Physics of Rainclouds*, Cambridge Univ. Press, New York, 1962.

Garten, V. A., and R. B. Head, Carbon particles and ice nucleation, *Nature*, *201*, 1091–1092, 1964.

Garten, V. A., and R. B. Head, A theoretical basis of ice nucleation by organic crystals, *Nature*, *205*, 160–162, 1965.

Haag, W., B. Kärcher, S. Schäfers, O. Stetzer, O. Möhler, U. Schurath, M. Krämer, and C. Schiller, Numerical simulations of homogeneous freezing processes in the aerosol chamber AIDA, *Atmos. Chem. Phys.*, *3*, 195–210, 2003.

Heintzenberg, J., K. Okada, and J. Ström, On the composition of non-volatile material in upper tropospheric aerosols and cirrus crystals, *Atmos. Res.*, *41*, 81–88, 1996.

Heymsfield, A. J., and L. M. Miloshevich, Homogeneous ice nucleation and supercooled liquid water in orographic wave clouds, *J. Atmos. Sci.*, *50*, 2335–2353, 1993.

Heymsfield, A. J., and R. M. Sabin, Cirrus crystal nucleation by homogeneous freezing of solution droplets, *J. Atmos. Sci.*, *46*, 2252–2264, 1989.

Heymsfield, A. J., L. M. Miloshevich, C. Twohy, G. Sachse, and S. Oltmans, Upper tropospheric relative humidity observations and implications for cirrus ice nucleation, *Geophys. Res. Lett.*, *25*, 1343–1346, 1998.

Hung, H.-M., A. Malinowski, and S. T. Martin, Kinetics of heterogeneous ice nucleation on the surfaces of mineral dust cores inserted into aqueous ammonium sulfate particles, *J. Phys. Chem. A*, *107*, 1296–1306, 2003.

Jensen, E. J., and O. B. Toon, The potential effects of volcanic aerosols on cirrus cloud microphysics, *Geophys. Res. Lett.*, *19*, 1759–1762, 1992.

Jensen, E. J., and O. B. Toon, The potential impact of soot particles from aircraft exhaust on cirrus clouds, *Geophys. Res. Lett.*, *24*, 249–252, 1997.

Jensen, E. J., et al., Ice nucleation processes in upper tropospheric wave-clouds observed during SUCCESS, *Geophys. Res. Lett.*, *25*, 1363–1366, 1998.

Kärcher, B., Contrails: Observations, formation mechanisms, atmospheric impacts, uncertainties, *Rep. 2000-01*, 47 pp., Dtsch. Zent. für Luft- und Raumfahrt, Cologne, Germany, 2000.

Kärcher, B., Properties of subvisible cirrus clouds formed by homogeneous freezing, *Atmos. Chem. Phys.*, *2*, 161–170, 2002.

Kärcher, B., and U. Lohmann, A parameterization of cirrus cloud formation: Homogeneous freezing of supercooled aerosols, *J. Geophys. Res.*, *107*(D2), 4010, doi:10.1029/2001JD000470, 2002a.

Kärcher, B., and U. Lohmann, A parameterization of cirrus cloud formation: Homogeneous freezing including effects of aerosol size, *J. Geophys. Res.*, *107*(D23), 4698, doi:10.1029/2001JD001429, 2002b.

Kärcher, B., and S. Solomon, On the composition and optical extinction of particles in the tropopause region, *J. Geophys. Res.*, *104*, 27,441–27,459, 1999.

Kärcher, B., T. Peter, U. M. Biermann, and U. Schumann, The initial composition of jet condensation trails, *J. Atmos. Sci.*, *53*, 3066–3083, 1996.

Khvorostyanov, V. I., and J. A. Curry, A new theory of heterogeneous ice nucleation for application in cloud and climate models, *Geophys. Res. Lett.*, *27*, 4081–4084, 2000.

Koop, T., B. P. Luo, A. Tsias, and T. Peter, Water activity as the determinant for homogeneous ice nucleation in aqueous solutions, *Nature*, *406*, 611–614, 2000a.

Koop, T., A. Kapilashrami, L. T. Molina, and M. J. Molina, Phase transitions of sea-salt/water mixtures at low temperatures: Implications for ozone chemistry in the polar marine boundary layer, *J. Geophys. Res.*, *105*, 26,393–26,402, 2000b.

Lin, H., K. J. Noone, J. Ström, and A. J. Heymsfield, Small ice crystals in cirrus clouds: A model study and comparison with in situ observations, *J. Atmos. Sci.*, *55*, 1928–1939, 1998.

Lin, R. F., D. O. Starr, P. J. DeMott, R. Cotton, K. Sassen, E. Jensen, B. Kärcher, and X. Liu, Cirrus parcel model comparison project phase 1: The critical components to simulate cirrus initiation explicity, *J. Atmos. Sci.*, *59*, 2305–2329, 2002.

Lohmann, U., Possible aerosol effects on ice clouds via contact nucleation, *J. Atmos. Sci.*, *59*, 647–656, 2002.

Lohmann, U., and B. Kärcher, First interactive simulations of cirrus clouds formed by homogeneous freezing in the ECHAM general circulation model, *J. Geophys. Res.*, *107*(D10), 4105, doi:10.1029/2001JD000767, 2002.

Lohmann, U., and B. Kärcher, Impact of the Mt. Pinatubo eruption on cirrus clouds formed by homogeneous freezing in the ECHAM general circulation model, *J. Geophys. Res.*, *108*, doi:10.1029/2002JD003185, in press, 2003.

Martin, S. T., Phase transitions of aqueous atmospheric particles, *Chem. Rev.*, *100*(9), 3403–3453, 2000.

Minikin, A., A. Petzold, J. Ström, R. Krejci, M. Seifert, P. van Velthoven, H. Schlager, and U. Schumann, Aircraft observations of the upper tropospheric fine particle aerosol in the Northern and Southern Hemispheres at midlatitudes, *Geophys. Res. Lett.*, *30*(10), 1503, doi:10.1029/2002GL016458, 2003.

Möhler, O., O. Stetzer, S. Schaefers, M. Krämer, A. Mangold, P. Budz, P. Zink, J. Schreiner, K. Mauersberger, W. Haag, B. Kärcher, and U. Schurath, Experimental investigations of homogeneous freezing of sulphuric acid particles in the aerosol chamber AIDA, *Atmos. Chem. Phys.*, *3*, 211–223, 2003.

Murphy, D. M., D. S. Thomson, and M. J. Mahoney, Organics, meteoritic material, mercury, and other elements in high altitude aerosols, *Science*, *282*, 1664–1669, 1998.

Pruppacher, H. R., and J. D. Klett, *Microphysics of Clouds and Precipitation*, Kluwer Acad., Norwell, Mass., 1997.

Rogers, D. C., P. J. DeMott, S. M. Kreidenweis, and Y. Chen, Measurements of ice nucleating aerosols during SUCCESS, *Geophys. Res. Lett.*, *25*, 1383–1386, 1998.

Sassen, K., and S. Benson, Ice nucleation in cirrus clouds: A model study of the homogeneous and heterogeneous modes, *Geophys. Res. Lett.*, *27*, 521–524, 2000.

Sassen, K., and B. S. Cho, Subvisual-thin cirrus lidar dataset for satellite verification and climatological research, *J. Appl. Meteorol.*, *31*, 1275–1285, 1992.

Sassen, K., and G. C. Dodd, Haze particle nucleation simulation in cirrus clouds and application for numerical and lidar studies, *J. Appl. Sci.*, *46*, 3005–3014, 1989.

Schröder, F., B. Kärcher, M. Fiebig, and A. Petzold, Aerosol states in the free troposphere at northern midlatitudes, *J. Geophys. Res.*, *107*(D21), 8126, doi:10.1029/2000JD000194, 2002.

Seifert, M., J. Ström, R. Krejci, A. Minikin, A. Petzold, J.-F. Gayet, U. Schumann, and J. Ovarlez, In situ observations of aerosol particles remaining from evaporated cirrus crystals: Comparing clean and polluted air masses, *Atmos. Chem. Phys. Discuss.*, *2*, 1599–1633, 2002.

Spice, A., D. W. Johnson, P. R. A. Brown, A. G. Darlison, and C. P. R. Saunders, Primary ice nucleation in orographic cirrus clouds: A numerical simulation of the microphysics, *Q. J. R. Meteorol. Soc.*, *125*, 1637–1667, 1999.

Ström, J., and S. Ohlsson, Real-time measurement of absorbing material in contrail ice using a counterflow virtual impactor, *J. Geophys. Res.*, *103*, 8737–8741, 1998.

Ström, J., B. Strauss, T. Anderson, F. Schröder, J. Heintzenberg, and P. Wendling, In situ observations of the microphysical properties of young cirrus clouds, *J. Atmos. Sci.*, *54*, 2542–2553, 1997.

Tabazadeh, A., and O. B. Toon, The role of ammoniated aerosols in cirrus cloud nucleation, *Geophys. Res. Lett.*, *25*, 1379–1382, 1998.

Twohy, C. H., and B. W. Gandrud, Electron microscope analysis of residual particles from aircraft contrails, *Geophys. Res. Lett.*, *25*, 1359–1362, 1998.

Vali, G., Atmospheric ice nucleation—A review, *J. Rech. Atmos.*, *19*, 105–115, 1985a.

Vali, G., Nucleation terminology, *J. Aerosol Sci*, *16*, 575–576, 1985b.

Wallace, J. M., and P. V. Hobbs, *Atmospheric Science*, Academic, San Diego, Calif., 1977.

Winker, D. M., and C. R. Trepte, Laminar cirrus observed near the tropical tropopause by LITE, *Geophys. Res. Lett.*, *25*, 3351–3354, 1998.

Wyslouzil, B. E., K. L. Carleton, D. M. Sonnenfroh, and W. T. Rawlins, Observation of hydration of single, modified carbon aerosols, *Geophys. Res. Lett.*, *21*, 2107–2110, 1994.

Zuberi, B., A. K. Bertram, T. Koop, L. T. Molina, and M. J. Molina, Heterogeneous freezing of aqueous particles induced by crystallized $(NH_4)_2SO_4$, ice, and letovicite, *J. Phys. Chem. A.*, *105*, 6458–6464, 2001.

Zuberi, B., A. K. Bertram, C. A. Cassa, L. T. Molina, and M. J. Molina, Heterogeneous nucleation of ice in $(NH_4)_2SO_4$-H_2O particles with mineral dust immersions, *Geophys. Res. Lett.*, *29*(10), 1504, doi:10.1029/2001GL014289, 2002.

B. Kärcher, Deutsches Zentrum für Luft- und Raumfahrt Oberpfaffenhofen, Institut für Physik der Atmosphäre, Postfach 1116, D-82234 Wessling, Germany. (bernd.kaercher@dlr.de)

U. Lohmann, Department of Physics and Atmospheric Science, Dalhousie University, Lord Dalhousie Drive, Halifax, Nova Scotia, Canada B3H 3J5. (Ulrike.Lohmann@dal.ca)